ACS OMEGA

http://pubs.acs.org/journal/acsodf

Article

Alkyl Silica Hybrid Nanowire Assembly in Improved Superhydrophobic Membranes for RO Filtration

Sahar Tasleem, Aneeqa Sabah,* Maryam Tahir, Aneela Sabir, Ammara Shabbir, and Mohsin Nazir

Cite This: https://doi.org/10.1021/acsomega.1c04498

Read Online

ACCESS | Metrics & More | Article Recommendations

ABSTRACT: Alkyl silica membranes and wires were synthesized by a sol−gel method, which has the capacity to control the size of the particles or membranes by controlling the reactions. Trimethoxyoctylsilane (C_8TMOS) was used as a chemical surfactant; poly(vinylpyrrolidone) (PVP) as an emulsifier, dissolved in butanol for emulsion; and tetraethylorthosilicate (TEOS) as a precursor and a source of silica. An assembly of silica wires was fabricated on glass and cotton substrates by the dip-coating technique. Porous membranes and silica wires were observed using scanning electron microscopy (SEM) images. The contact angles of all of the samples were in the range of 140−154° as measured by ImageJ software, which confirmed the hydrophobic nature of the samples. The contact angle was increased by increasing the amount of the surfactant. Phase changes of silica wires and membranes were investigated by thermogravimetric analysis. Chemical bonds of the sample were studied using Fourier transform infrared (FTIR) spectroscopy. The band gap of silica nanowires was measured to be 3.8−3.4 eV using the UV−visible spectrum and decreased as compared to that of bulk silica. These silica-based porous membranes with enhanced transport properties can be used in filtration and separation techniques. This fabricated hybrid silica membrane showed ∼96% salt rejection within a permeation flux of 3.04 L/m^2 h.

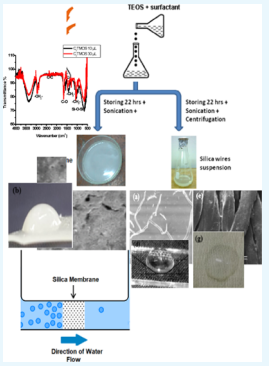

INTRODUCTION

Membrane separation technology has developed rapidly over recent years because it is a low-cost and energy-efficient process compared to other filtration techniques. Silica membranes have good physical and chemical processes compared to other filtration techniques. Silica membranes have good physical and chemical properties with unique thermal and structural stabilities. Silica particles are very attractive additives and fillers for altering surface properties through functionalization.[1,2] Initially, silica is hydrophilic due to the presence of silanol (Si−OH) groups on the surface of the particle. This hydrophilic additive destabilizes the dopant solution, thereby enhancing the viscosity and kinetic effect to promote the formation of highly modified porous membranes.[3,4]

Silica membranes synthesized by the sol−gel method[5] result in higher selectivity, controlled pore size, and a relatively thin (100 nm or less) separation layer, which is necessary to obtain high permeability. The two main routes in the sol−gel synthesis, the colloidal route and the polymeric route were, followed in membrane synthesis. Sol−gel is a facile technique that allows for a variety of binary, tertiary, and complex chemical compositions of ligands and networks resulting in organic and inorganic hybrid materials.[6] Modification of ion exchange membranes with nanoparticles leads to significant changes in transport properties of membranes via pores and channel systems. Formation of nanoparticles into pores changes the pore size and volume, thus enhancing the transport of even smaller ions and molecules through hybrid membranes.[7] Emerging membrane technologies are highly attractive for wastewater purification with higher efficiency.[8−10] Membrane flux can be controlled by surface properties and the number and size of pores on the surface.[11−13] The pore size formation is strongly affected by polymer-based solvent interactions, chain strength, arrangement, and entanglement that occur during initial phase changes through the reaction.[14,15] Highly porous membranes can be developed mostly by incorporation of pores through hydrophilic polymeric additives such as poly(vinylpyrrolidone) (PVP), poly(ethylene glycol), etc.[16−19] These additives destabilize the dope solution, which results in demixing, and thus promote the formation of highly porous membranes.[20,21] Silica particles are more attractive additives as we can change their surface properties by functionalization. Inclusion of silica particles can significantly enhance the viscosity to increase the kinetic effect during phase changes.[22,23] Addition of hydrophilic silica particles can increase the pore size, porosity, and wettability.[24]

Very limited literature is available for the use of silica as an additive for membrane fabrication. This work explains the role of silica in upgrading the surface pore formation, size, and

Received: August 18, 2021
Accepted: January 13, 2022

performance of membranes. The wettability of fabricated silica wires was tested on various substrates such as glass and cotton fabrics. Agent concentration has a strong influence on the thermal properties of cotton fabric. Cotton fabric exhibited thermal degradation due to pyrolysis by two pathways: (i) the decomposition of the glycol units at low temperatures and (ii) the depolymerization of burning units into volatile products containing levoglucosan at high temperatures.[25] The miscibility of polymers and copolymers is reported to investigate the thermal degradation and stability with density variations.[26,27] The literature revealed the thermal stability of coated cotton fabric by annealing at various temperatures ranging from 50 to 300 °C under ambient conditions.[28] Poly(vinylpyrrolidone) (PVP) is a water-soluble polymer obtained by polymerization of monomer *N*-vinyl pyrrolidone. PVP is an inert, nontoxic, temperature-resistant, pH-stable, biocompatible, and biodegradable polymer that helps us to encapsulate and stabilize silica particles and membranes. The performance of fabricated membranes was tested for salt filtration. A key challenge is to fabricate modified and highly functionalized metal-doped hydrophobic silica nanoparticles and membranes by the simple and facile sol−gel technique.

RESULTS AND DISCUSSION

FTIR Spectrum of the Samples. Fourier transform infrared (FTIR) spectroscopy was performed using an IRTracer-100 FTIR spectrometer in the 4000−400 cm^{-1} range, and the resulting spectra are shown in Figure 1. The

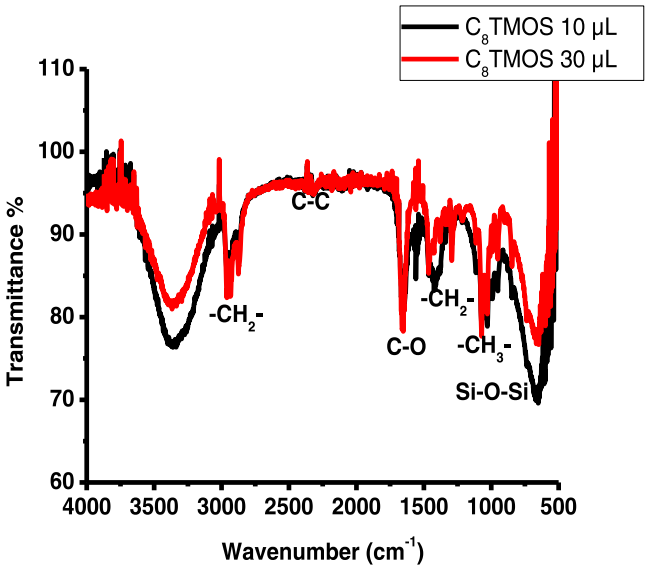

Figure 1. Comparison graph of FTIR spectra for samples prepared by 10 and 30 μL of trimethoxyoctylsilane.

spectra formed by molecular adsorption of IR radiation by silica wires that form molecular imprints of the sample, which are ascribed to different vibrations, are shown in Table 1. For 10 μL of C_8TMOS, the peak at 3347 cm^{-1} is attributed to the sharp and strong O−H stretching vibration of H_2O in the sample,[5,28] which is due to the fact that silica particles have a tendency to absorb water from the atmospheric air. The peaks at 2958 and 2855 cm^{-1} are attributed to the symmetric and asymmetric stretching vibrations of the C−H group, respectively.[32,33] The peak at 1659 cm^{-1} is ascribed to the imide C═O stretching and that at 1462 cm^{-1} is due to the

Table 1. Characteristic Vibrational Frequencies (cm^{-1}) in FTIR Spectra of Hybrid Silica Wires (SiWs) Synthesized with Two Different Concentrations of Surfactant C_8TMOS, i.e., 10 and 30 μL

	SiWs prepared using surfactant concentration			
no.	10 μL	30 μL	types of vibrations	structural units
1	3366	3366	O−H stretching and SiO−H	H−O−H···H_2O and ≡SiO−H···H_2O
2	2963	2963	ν_sC−H	$-CH_3$
3	2933	2949	ν_{as}C−H	$-CH_2$
4	2881	2881	ν_{as}C−H	$-CH_3$
5	2168	2210	C−C stretching	C−C
6	2115	2115	a combination of hindered rotation and O−H bending of water	H−O−H
7	1656	1656	C ═ O stretching	C═O
8	1422		δ_{as}C−H	Si−R
9	1478	1380	δ_sC−H	$-CH_2$
10	1297	1297	δ_sC−H	Si−R
11	1219	1219	CH_2 wagging vibrations	$-CH_2$
12	1114	1114	asymmetric vibrations of ν_{as}Si−O−Si	≡O−Si−O≡
13	1048		ν_{as}Si−O−Si (TO mode)	≡O−Si−O≡
14	928		ν_βSi−O	≡Si−OH
15	847	847	νSi−C	Si−R
16	1048, 732	1047, 870	stretching	Si−O−Si
17	594	594 (noise)	νSi−O	SiO_2 defects
18	556	556 (noise)	νSi⬡−O	SiO_2 defects

bending of $-CH_2-$. The peak at 1387 cm^{-1} is assigned to the C−H symmetric deformation vibrations (bending) of $-CH_2$ groups and that at 1294 cm^{-1} is attributed to the silicon-bonded alkyl-group C−H bending. The band at 1040 cm^{-1} corresponds to asymmetric stretching vibrations of O−Si−O.[34,35] The peak at 928 cm^{-1} is assigned to the Si−OH bond, whereas the one appearing at 846 cm^{-1} corresponds to the symmetric stretching vibrations of O−Si−O for the prepared sample.[36] The very feeble peak at 741 cm^{-1} is ascribed to CH_2 rocking vibrations.[37] These bands are very important, and especially those at 1040, 928, and 846 cm^{-1} confirm the presence of silica even without the surfactant. The peak at 2942 cm^{-1} is attributed to the asymmetric stretching vibration of the $-CH_2-$ bond. The next peak, which was broad and intense, at 2168 cm^{-1} showed the C−C bond. The peak at 1658 cm^{-1} is attributed to C−O bonding. The peaks at 1421 and 1326 cm^{-1} showed the symmetric vibrations of $-CH_2-$ and $-CH_3-$, respectively. Then, the peaks from 1048 to 732 cm^{-1} indicated the stretching vibrations of the Si−O−Si bond.[36] When the samples with 30 μL of C_8TMOS were analyzed, they showed a peak at 2949 cm^{-1}, indicating the asymmetric stretching vibration of the $-CH_2-$ bond.[38] The next peak, which was broad and intense, at 2210 cm^{-1} showed the C−C bond. The peak at 1654 cm^{-1} is attributed to C−O bonding. The peaks at 1478 and 1308 cm^{-1} showed the symmetric vibrations of $-CH_2-$ and $-CH_3-$, respectively. Then, the peaks from 1047 to 870 cm^{-1} indicated the stretching vibrations of Si−O−Si end grouping.[39]

Thermogravimetric Analysis. Thermal analysis (TGA, DSC) of silica wires was carried out using a Q 600 (TA

https://doi.org/10.1021/acsomega.1c04498
ACS Omega XXXX, XXX, XXX−XXX

Instruments) in an inert atmosphere under a flow of argon gas at a heating rate of 15 °C/min. Thermal properties such as weight loss at different temperatures were studied using the thermogravimetric analysis of samples shown in Figure 3. The TGA curve of samples prepared by 10 μL of C_8TMOS showed a weight loss of 13.4% at 288.9 °C corresponding to two endothermic peaks in the differential scanning calorimetry (DSC) curve at 132.8 and 193.8 °C, respectively. This initial weight loss is attributed to the evaporation of the solvent, i.e., ethanol.[40] The same sample showed a further weight loss of 11.1% at 457.2 °C corresponding to exothermic peaks in the DSC curve at 516 °C. This later weight loss is due to the decomposition of the alkyl $-CH_3-$ group.[3]

The TGA curve of samples prepared by 30 μL of C_8TMOS showed a weight loss of 12.5% up to 290.5 °C corresponding to endothermic peaks at 136.4 and 192 °C in the DSC curve. Then, a larger and rapid weight reduction of 38.8% was seen up to 497.6 °C corresponding to endothermic peaks at 316.7 and 454.8 °C in the DSC curve, which is attributed to the evaporation of the solvent, i.e., ethanol. Between 497.6 and 671 °C, there was only a slight decrease of 3.8% in weight, corresponding to an exothermic peak at 578.6 °C in the DSC curve, which is due to the decomposition of the alkyl $-CH_3-$ group in the synthesized sample. An endothermic peak at 457.2 °C also showed the melting of the sample, indicating the change in its physical state from solid to liquid.[4] The thermal stability of the sample is seen after 500 °C as depicted in Figure 2.

Contact Angle of Silica Nanomembranes. The prepared NW membranes were hydrophobic with a contact angle of 145 and 154° for 10 and 30 μL of trimethoxyoctylsilane (C_8TMOS), respectively, as measured using a digital camera microscope (Figure 3a–c). This is because the C_8 group of the surfactant shielded the building blocks of the NW membrane. This revealed that the wettability of the membrane decreased because the contact angle increased. The increased amount of surfactant leads to superhydrophobicity and a decrease in wettability.

Contact Angle of Silica NWs on Glass Substrate. Silica NWs were coated on a glass slide with 10 and 30 μL of trimethoxyoctylsilane (C_8TMOS) as the surfactant, presenting a contact angle of 140 and 153°, respectively, to confirm hydrophobicity (Figure 3c,d). Water droplets created a high-energy wall to form a liquid–solid boundary on the exterior surface. Moreover, the macropores in the networks of the NWs can set up air inside, providing an air pad to hang the drops of water. The increasing amount of surfactant increased the contact angle making the wires superhydrophobic.[41]

Contact Angle of Silica NWs on Cotton Fabric. The contact angle of silica nanowires on cotton fabric with 10 μL of trimethoxyoctylsilane (C_8TMOS) as surfactant is 135°, confirming the hydrophobic property. The water-repellent ability of the coated surface can be credited to the result of nanosized silica particles and the hydrophobic characteristic of the alkyl silane agent, which in this case is the surfactant. The sample with 30 μL of trimethoxyoctylsilane (C_8TMOS) as surfactant has a contact angle of 145°, which showed that by increasing the amount of surfactant the contact angle increases.[6]

UV–Vis Spectroscopy. The UV–vis absorption spectrum of the prepared silica nanoparticles dispersed in ethanol was obtained using a U-2800 Hitachi UV–vis spectroscope.

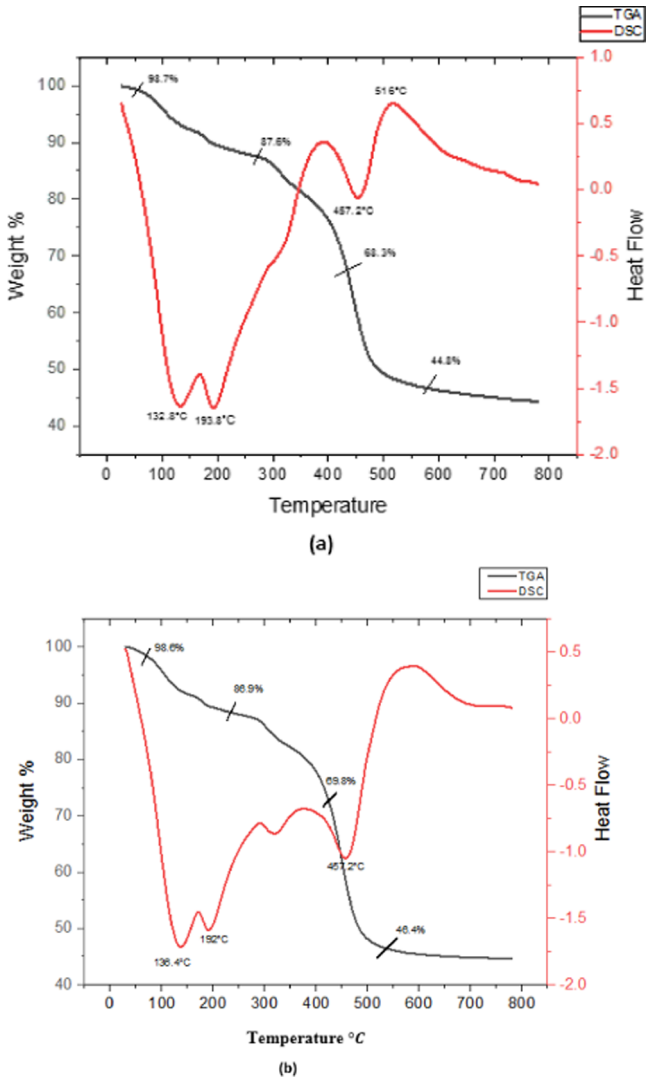

Figure 2. TGA/DSC curves of samples prepared by (a) 10 μL of C_8TMOS and (b) 30 μL of C_8TMOS.

UV–Vis Analysis of Silica Nanowires with Trimethoxyoctylsilane. The UV–vis spectrum of the sample synthesized with 10 μL of C_8TMOS represented a strong absorption peak at 276 nm, and the sample with 30 μL of C_8TMOS presented a peak at 280 nm, which is in the range of the absorption peak of silica nanoparticles as shown in Figure 4. These wavelengths showed that the prepared sample with 30 μL of C_8TMOS was red-shifted from 10 μL of C_8TMOS. The red shift indicated the increase in the size of the particles. On increasing the amount of surfactant, the value of absorbance increased. This is in accordance with Beer–Lambert's law which states that the value of absorbance increases on increasing the concentration of nanoparticles in the solution.[7]

Band Gap. Using the Planck–Einstein equation, the relationship between band gap energy and wavelength is given as

$$E_g = h_\upsilon = h_c/\lambda$$

In this equation, E_g is the band gap energy in eV, h is Planck's constant, λ is the wavelength, and c is the speed of light.[8] The band gap can be calculated by plotting a graph between photon energy in eV and $(\alpha h\nu)^2$. Using Tauc's plot, the optical band

https://doi.org/10.1021/acsomega.1c04498
ACS Omega XXXX, XXX, XXX–XXX

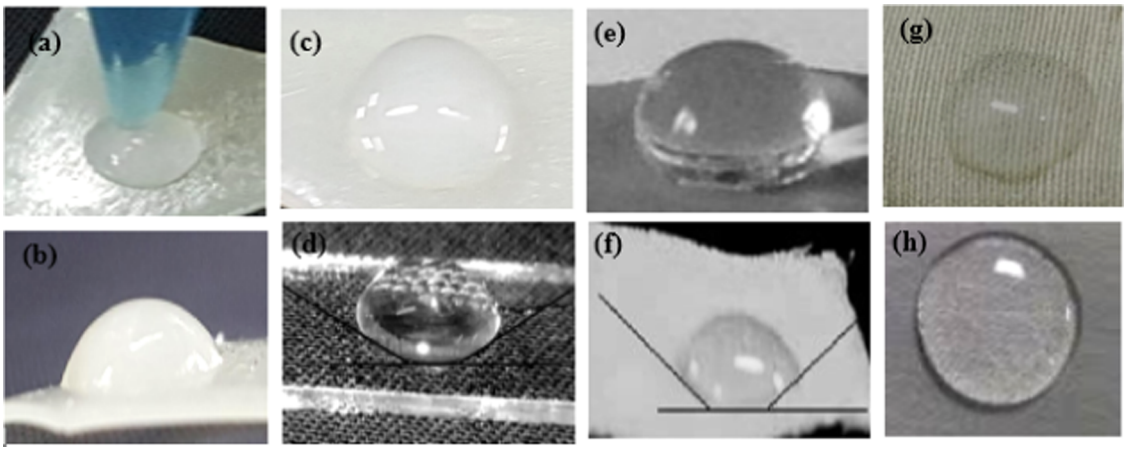

Figure 3. Contact angle measurements for 10 and 30 μL of trimethoxyoctylsilane (C_8TMOS) water droplets on substrates: (a) water droplet on silica membrane, (b, c) M10: 145° and M30: 154° on a membrane, (d, e) G10: 140° and G30: 153° for glass, and (f–h) C10: 135° and C30: 145°.

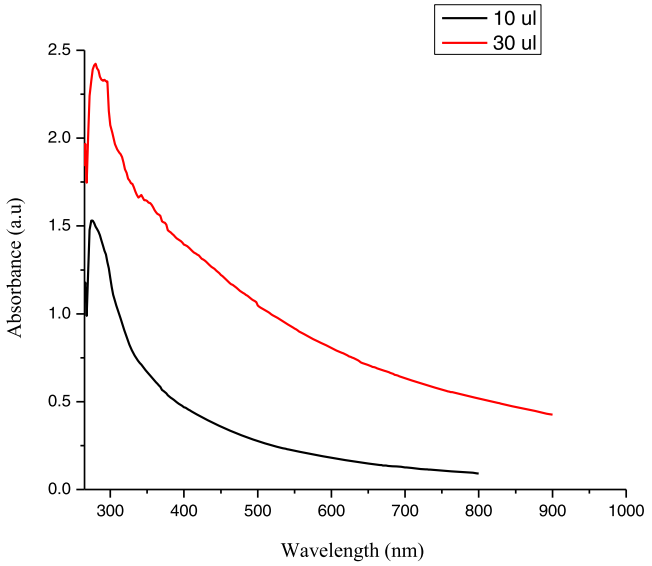

Figure 4. UV–vis absorption spectrum of silica nanomembranes with 10 and 30 μL of C_8TMOS.

gap was calculated by drawing a tangent on the axis of photon energy.

The band gap of SiO_2 with 10 and 30 μL of C_8TMOS was calculated to be 3.8 and 3.4 eV, respectively, as shown in Figure 5. The band gap was reduced because there was an increase in particle size, which predicted the size-dependent energy gap.[9]

Morphological Analysis. Morphological analysis was performed using a Jeol SEM JSM-6480LV to visualize silica wires on various substrates and their self-assembly into membranes.

SEM of Silica NWs on Glass Substrate. Figure 6a,b shows the scanning electron microscopy (SEM) images of silica wires coated on glass substrate by dip-coating before and after sonication, Figure 6c,d, of silica suspension, respectively. A network of 3D superhydrophobic silica wires with a snakelike slim structure consisting of a less-bright Si core covered with a brighter silicon oxide shell was observed.[10] The chemically inert Si oxide shell prohibited the lateral growth of Si wires; thus, their perpendicular growth resulted in the branched structure of the material as observed. The sample prepared using 30 μL of surfactant showed a more self-assembled porous structure of silica wires than that prepared using 10 μL. The more closely packed porous mesh of silica wires in the former sample, synthesized with a higher concentration of surfactant, resulted in a hierarchal surface ensuring the improved

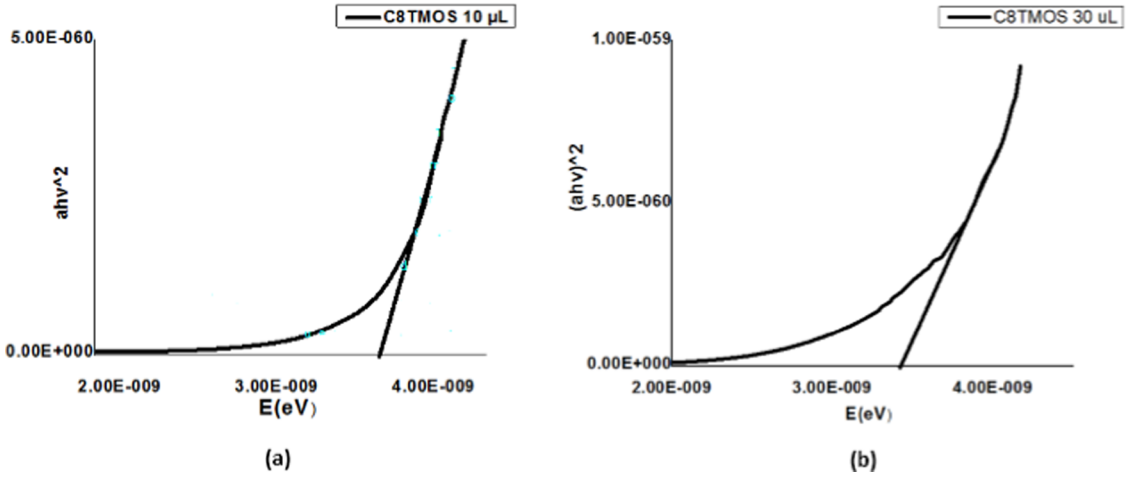

Figure 5. Optical band gap spectrum of silica nanomembranes with (a) 10 μL and (b) 30 μL of C_8TMOS.

https://doi.org/10.1021/acsomega.1c04498
ACS Omega XXXX, XXX, XXX–XXX

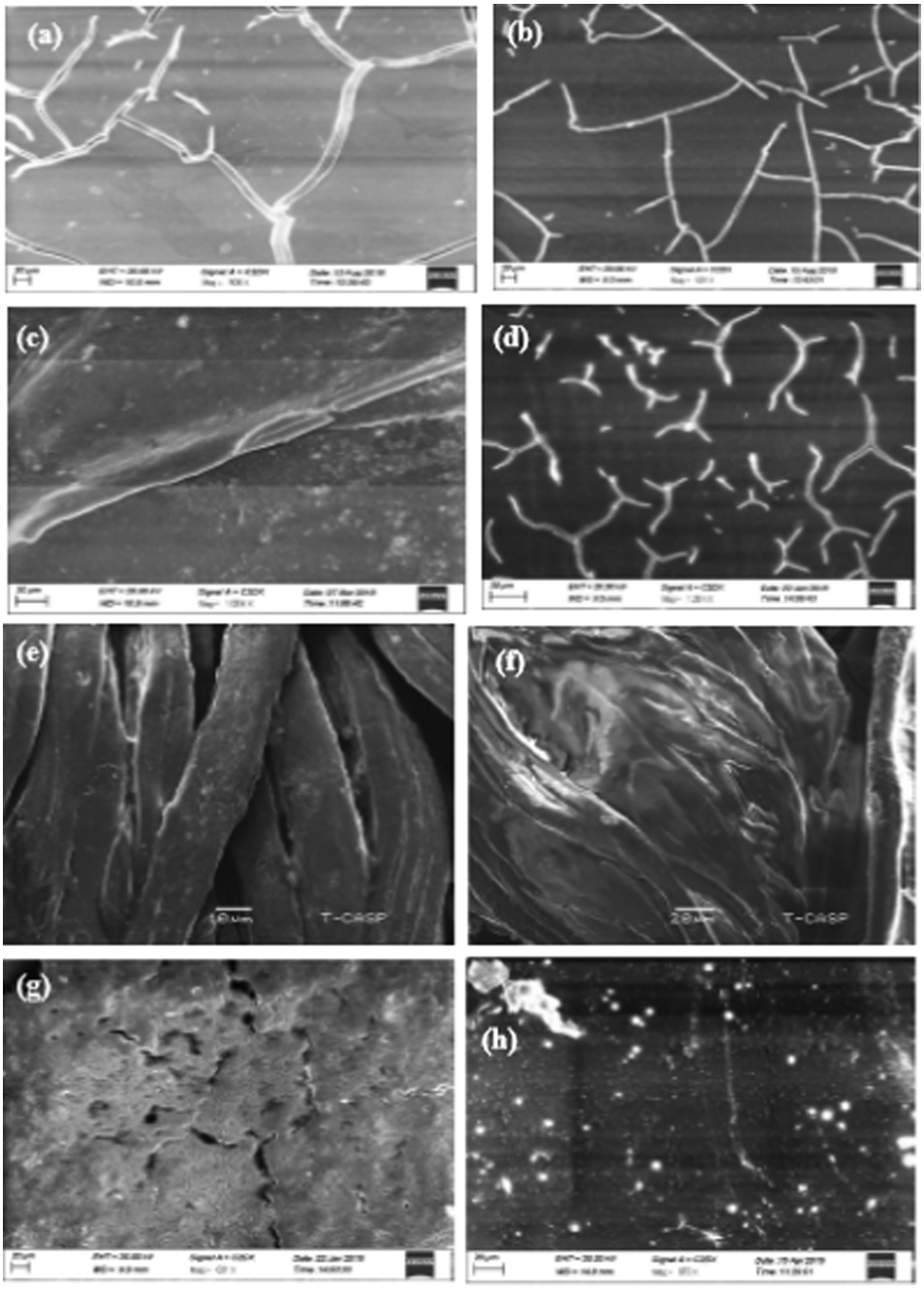

Figure 6. SEM images of silica wires prepared (a, b) without sonication with 10 and 30 μL of C_8TMOS on a glass substrate, (c, d) after sonication with 10 and 30 μL of C_8TMOS on a glass substrate, (e, f) with 10 and 30 μL of C_8TMOS on cotton fabric, and (g, h) with 10 and 30 μL of C_8TMOS on a nanomembrane.

hydrophobicity as verified by water contact angle measurements of ∼140 and 153°. The SEM images of silica wires were obtained after the sonication process, resulting in tadpolelike 3D structures that were superhydrophobic.[11]

SEM of Silica NWs on Cotton Fabric. The morphology of cotton fabrics treated with silica wire samples synthesized with two different concentrations of 10 and 30 μL of surfactant trimethoxyoctylsilane (C_8TMOS), respectively, was observed using SEM images as shown in Figure 6e,f. The tiny particles of silica attached to fabric fibers contributed to the roughness, thus making the surface of the fabric more hydrophobic. The water repellency of the fabric was also evident by the contact angle measurement as discussed earlier. An increase in the concentration of surfactant can increase adsorption on cotton fabric and decrease the adhesion force, thus reducing the wetting ability of the fabric beyond the critical micelle concentration.[12]

SEM of Silica Nanomembranes. SEM images of hybrid silica membranes prepared using 10 and 30 μL of surfactant C_8TMOS revealed porous structures. These pores give rise to the hierarchal structure of the surface of the membranes and make them fairly rough by the arrangement of tiny air pockets within them, as shown in Figure 6g,h, thus contributing to superhydrophobicity.[13] The closely packed porous network

https://doi.org/10.1021/acsomega.1c04498
ACS Omega XXXX, XXX, XXX−XXX

obtained by increasing the amount of surfactant (30 μL) resulted in a rougher surface and increased superhydrophobicity as confirmed by contact angle measurements.[14] SEM images revealed the wirelike network of silica for C_8TMOS as compared to the scattered silica particles in SDS. Therefore, for further research, C_8TMOS was chosen as a closed network surface structure, and it was rough enough to achieve better hydrophobicity.

Silica Membrane Performance Test for Flux and $MgSO_4$ Rejection by Reverse Osmosis RO Filtration. The hybrid silica membrane prepared by 10 μL of surfactant trimethoxyoctylsilane (C_8TMOS) showed 95.9% capability of $MgSO_4$ rejection at a permeate flux of 3.04 L/m^2 h whereas that prepared by 30 μL of surfactant resulted in a salt rejection capability of 96.8% with a 2.83 L/m^2 h permeate flux as performed by RO filtration plant (Hp 470 sterlith company deadend) in Georgia Institute of Technology. Schematics are shown in Figure 7.

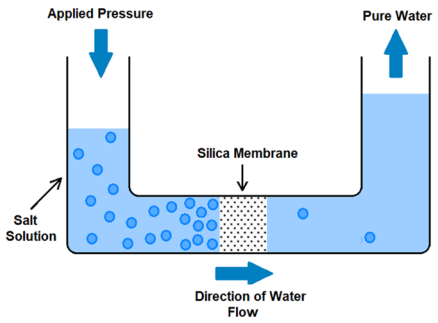

Figure 7. Schematics of reverse osmosis RO filtration of $MgSO_4$ salt rejection by C_8TMOS silica membranes.

The higher salt rejections were observed in the case of higher surfactant concentration (30 μL) as compared to the lower surfactant amount used in the synthesis of hybrid silica membranes. This is due to the fact that in the former case, a closely packed mesh of silica was formed in membranes due to the higher silica concentration, which caused smaller pores to be a hurdle to salt diffusion. However, poor flow dynamics consequently improved salt rejection resulting in a lower permeate flux of the prepared sample. This is due to hydrophobic membranes avoiding the diffusion of aqueous solution into the pores due to the difference in silica membrane pore sizes and those of salt molecules.[16]

EXPERIMENTATION

Synthesis of Silica Films on Glass and Fabric. In a typical synthesis, 2 g of PVP (C_6H_9NO) used as a precursor was dissolved in 20 mL of *n*-butanol. The mixture was stirred using a magnetic stirrer at 450−500 rpm for 10 min. Then, 2 mL of ethanol, 0.56 mL of distilled water, 1.36 mL of sodium citrate ($Na_3C_6H_5O_7$), and 0.4 mL of ammonia solution were added sequentially to the above solution. The mixture was hand-shaken for 2−3 min after addition of each chemical. Furthermore, the mixture was divided equally into two flasks, and in each flask, 100 μL of TEOS was added. C_8TMOS was added to the two flasks with two different concentrations of 30 and 60 μL, respectively, and shaken immediately for 5 min. Finally, the two solutions were left static for 24 h at room temperature with proper covering. A chemical surfactant trimethoxyoctylsilane (C_8TMOS):($C_{11}H_{26}O_3Si$) was added to the above mixture for cross-linkage between the water/oil medium and as a source of silica.[5,29]

After 24 h, the two solutions were placed in an ultrasonic bath cleaner for 1 h to remove the residues. Sonication was performed at 40 Hz, 35 °C, and 100 W. Then, the samples were centrifuged to separate the nanoparticles at 4500 rpm for 30 min. Suspensions of both samples were made in ethanol with a silica concentration of 20 mg/mL. The silica films were coated on glass slides by the dip-coating technique. A glass slide of dimension 3 cm × 1 cm was hung between the clips of the dip coater. The glass slide was immersed in the suspension at a constant speed, i.e., 300 rpm. After soaking for about 10−12 s in the suspension, the slide was then pulled out. On the glass slide, a thin layer of silica wires was deposited. The excess liquid was removed from the surface by shaking the glass slide for a few seconds.[30,31] The mixture was shaken for 5 min immediately and left static for 22 h at 37 °C to grow silica wires (SiWs). The sample was then sonicated (DSA100-SK1-2.8L, V = 220 V, P = 100 W, 50 Hz) for 1 h and centrifuged (PLC-3, P = 220 V/50 Hz, 0.65 A) at 4500 rpm for 60 min to separate SiWs in a 15 mL centrifugation tube. The hybrid SiWs were washed with ethanol, air-dried for 2 days, and finally used to prepare a suspension of 20 mg/mL silica in ethanol.[30] Samples denoted as S_1 and S_2 were obtained using two different amounts, i.e., 30 and 60 μL, of surfactant C_8TMOS by the above method. The silica films were coated on glass slides by the dip-coating method (as mentioned above) and cotton fabric by immersing the fabric in the final solution for 5 min with stirring and then drying in an oven at 80 °C for 3 min.

Synthesis of Silica Membranes. Hybrid silica membranes were synthesized using the same method as that mentioned for silica films, with the only difference being that the amount of poly(vinylpyrrolidone) (PVP $[C_6H_9NO]_n$) was doubled. PVP played the role of binding material for membrane function.[42] Polymer blending demonstrates a wide range of properties such as water solubility, binding, high solubility, and good thermal resistance depending on pH, concentration, and density variations.[43,44] The final solution was poured into a Petri dish and dried in an oven at 45 °C for 6 h, which resulted in very fine membranes. Schematics of the experiment are shown in Figure 8.

Chemical Reactions. Sodium citrate was used as a stabilizing agent, and an ammonia solution was added to maintain the pH of the solution. When they both reacted due to the presence of hydrogen ions in water, the solution became acidic. Sodium citrate produced citric acid and then ammonium citrate was formed, which showed that no more hydrogen ions were present in the solution.[36]

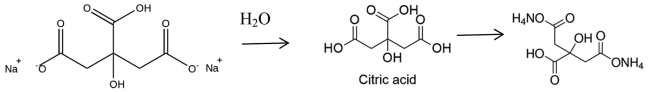

Preparation of Silica Nanoparticles. Tetraethylorthosilicate ($Si(OC_2H_5)_4$) reacted with water to form silanol groups. The following chemical reactions are involved in preparation of silica nanoparticles.Hydrolysis:

$$Si(OC_2H_5)_4 + H_2O \rightarrow Si(OC_2H_5)_3OH + C_2H_5OH$$

Water Condensation:

https://doi.org/10.1021/acsomega.1c04498
ACS Omega XXXX, XXX, XXX−XXX

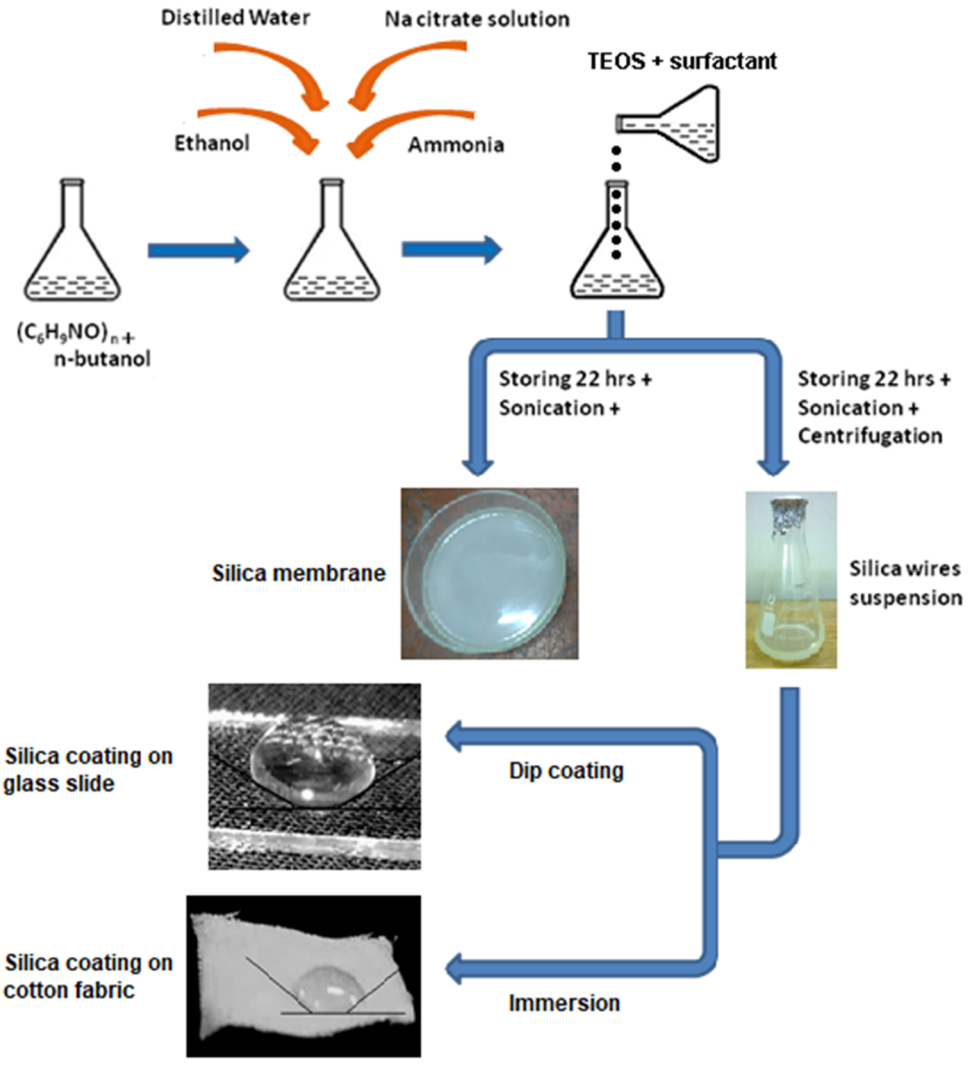

Figure 8. Schematic process for preparing transparent hybrid hydrophobic silica films by the sol−gel method on a glass substrate and cotton fabric with their self-assembly in the form of membranes.[a]Photos in Figures 3, 5, and 8 were taken by Maryam Tahir (author) and Dr. Aneeqa Sabah (corresponding author).

$$\equiv Si - O - H + H - O - Si \equiv \rightarrow \equiv Si - O - Si \equiv + H_2O$$

Alcohol Condensation:

$$\equiv Si - OC_2H_5 + H - O - Si \equiv \rightarrow \equiv Si - O - Si \equiv + C_2H_5OH\ [46]$$

The whole silica structure was made up of siloxane bridges (Si−O−Si) by the condensation/polymerization between the silanol groups or between ethoxy groups. The stages involved in the establishment of silica particles can be characterized by nucleation and growth.

The nucleated silica nanoparticles remained at the boundary of the droplets. The purpose of sodium citrate in the water droplets was to stabilize the hydrolyzed TEOS and to provide silica.

In the meantime, when in contact with simple water droplets, the trimethoxyoctylsilane C_8TMOS dissolved in the oil phase (*n*-butanol) and hydrolyzed into $C_8Si(O-)_3$. Prominently, $C_8Si(O-)_3$ had amphiphilic properties, i.e., it possesses both hydrophilic and lipophilic properties, with its hydrophilic $Si(O-)_3$ ion fronting the water phase and the C_8 tail toward the *n*-butanol solvent. The surface tension of the water droplet was reduced by interfacially arranged $C_8Si(O-)_3$ due to its role as a surfactant, which was in contact with the nucleated silica nanoparticles.[35]

CONCLUSIONS

Silica particles were successfully synthesized in the presence of trimethoxyoctylsilane (C_8TMOS) as surfactant. The effect of different amounts of surfactant on the composition, morphology, and optical properties was studied in detail. The FTIR results confirmed the presence of alkyl groups on the silica surface at 2942−2168 cm^{-1} and peaks from 1047 to 870 cm^{-1} indicated the stretching vibrations of the Si−O−Si bond. Silica films and membranes showed hydrophobic and superhydrophobic characters within contact angles in the range of 140−154°. The contact angle was increased by increasing the amount of surfactant. This was evident for all samples coated on different substrates such as glass slides and cotton fabric and also for samples of the membrane. TGA and DSC analysis showed the weight loss at different temperatures, and thermal stability of both samples was attained after 500 °C. An

https://doi.org/10.1021/acsomega.1c04498
ACS Omega XXXX, XXX, XXX−XXX

absorption peak at 276 and 280 nm and a band gap of 3.8 and 3.4 eV of 10 and 30 μL of C_8TMOS, respectively, were observed. The absorption spectra were increased by increasing the amount of the surfactant as the particle size increased. The silica wires and membranes on the coating of the sample on glass slides and the porous structure of the membrane were evident. The prepared membranes were used to filter $MgSO_4$ solution, and the membrane prepared using 10 μL of C_8TMOS showed a salt rejection capability of 95.9% and the membrane with 30 μL of C_8TMOS had a salt rejection capability of 96.8%. It is estimated that the synthesized membranes can be used for application in water purification with accuracy, and these membranes can be made antibacterial for use in different fields of science and technology.

AUTHOR INFORMATION

Corresponding Author

Aneeqa Sabah − *Physics Department, Lahore College for Women University, Lahore 54000, Pakistan;* orcid.org/0000-0002-3678-9985; Email: aneeqas29@gmail.com

Authors

Sahar Tasleem − *Physics Department, Lahore College for Women University, Lahore 54000, Pakistan;* orcid.org/0000-0003-0823-5237

Maryam Tahir − *Physics Department, Lahore College for Women University, Lahore 54000, Pakistan*

Aneela Sabir − *Polymer Engineering and Technology, Punjab University, Lahore 54000, Pakistan*

Ammara Shabbir − *Physics Department, FC College, Lahore 54600, Pakistan*

Mohsin Nazir − *Computer Science Department, Lahore College for Women University, Lahore 54000, Pakistan*

Complete contact information is available at: https://pubs.acs.org/10.1021/acsomega.1c04498

Notes

The authors declare no competing financial interest.

ACKNOWLEDGMENTS

The authors acknowledge the support of laboratory facilities provided by Central Lab Lahore College for Women University, LCWU, Lahore, Pakistan; Polymer Engineering and Technology Department, Punjab University, Lahore, Pakistan; and Georgia Institute of Technology.

REFERENCES

(1) MatNawi, N. I.; Chean, H. M.; Shamsuddin, N.; Bilad, M. R.; Narkkun, T.; Faungnawaki, K.; Khan, A. L. Development of hydrophilic PVDF membrane using vapour induced phase separation method produced water treatment. *Membranes* **2020**, *10*, No. 121.

(2) Fahrina, A.; Arahman, N.; Mulyati, S.; Aprilia, S.; MatNawi, N. I.; Aqsha, A.; Bilad, M. R.; Takagi, R.; Matsuyama, H. Development of polyvinylidene fluoride membrane by incorporating bio-based ginger extract as additive. *Polymers* **2020**, *12*, No. 2003.

(3) Bottino, A. Preparation and properties of novel organic−inorganic porous membranes. *Sep. Purif. Technol.* **2001**, *22*−*23*, 269−275.

(4) Mavukkandy, M. O.; Bilad, M. R.; Kujawa, J.; Al-Gharabli, S.; Arafat, H. A. On the effect of fumed silica particles on the structure, properties and application of PVDF membranes. *Sep. Purif. Technol.* **2017**, *187*, 365−373.

(5) Tasleem, S.; Sabah, A.; Cheema, A. U.; Sabir, A. Transparent hydrophobic hybrid silica films by green and chemical surfactants. *ACS Omega* **2019**, *4*, 13543−13552.

(6) Lei, Q.; Jimin, G.; Noureddine, A.; Wang, A.; Stefan Wuttke, S.; Jeffrey Brinker, C.; et al. Sol−Gel-based advanced porous silica materials for biomedical applications. *Adv. Funct. Mater.* **2020**, *30*, No. 1909539.

(7) Safronova, E. Y.; Yaroslavtsev, A. B. Prospects of practical application of hybrid membranes. *Pet. Chem.* **2016**, *56*, 281−293.

(8) Ismail, A. F.; Matsuura, T. *Sustainable Membrane Technology for Energy, Water, and Environment*; John Wiley & Sons, 2012.

(9) Baker, R. W. *Membrane Technology and Applications*, 3rd ed.; John Wiley & Sons: Chichester, West Sussex, U.K., 2012.

(10) Bilad, M. R.; Arafat, H. A.; Vankelecom, I. F. J. Membrane technology in microalgae cultivation and harvesting: a review. *Biotechnol. Adv.* **2014**, *32*, 1283−1300.

(11) Fane, A. G.; Fell, C. J. D.; Waters, A. G. The relationship between membrane surface pore characteristics and flux for ultrafiltration membranes. *J. Membr. Sci.* **1981**, *9*, 245−262.

(12) Gryta, M. Influence of polypropylene membrane surface porosity on the performance of membrane distillation process. *J. Membr. Sci.* **2007**, *287*, 67−78.

(13) Ziel, R.; Haus, A.; Tulke, A. Quantification of the pore size distribution (porosity profiles) in microfiltration membranes by SEM, TEM and computer image analysis. *J. Membr. Sci.* **2008**, *323*, 241−246.

(14) Vandezande, P.; Gevers, L. E. M.; Vankelecom, I. F. J. Solvent resistant nanofiltration: separating on a molecular level. *Chem. Soc. Rev.* **2008**, *37*, 365−405.

(15) Zhenxin, Z.; Matsuura, T. Discussions on the formation mechanism of surface pores in reverse osmosis, ultrafiltration, and microfiltration membranes prepared by phase inversion process. *J. Colloid Interface Sci.* **1991**, *147*, 307−315.

(16) Kim, I.-C.; Lee, K.-H. Effect of various additives on pore size of polysulfone membrane by phase-inversion process. *J. Appl. Polym. Sci.* **2003**, *89*, 2562−2566.

(17) Garcia-Ivars, J.; Alcaina-Miranda, M.-L.; Iborra-Clar, M.-I.; Mendoza-Roca, J.-A.; Pastor-Alcañiz, L. Enhancement in hydrophilicity of different polymer phaseinversion ultrafiltration membranes by introducing PEG/Al2O3 nanoparticles. *Sep. Purif. Technol.* **2014**, *128*, 45−57.

(18) Ma, Y.; Shi, F.; Wang, Z.; Wu, M.; Ma, J.; Gao, C. Preparation and characterization of PSf/clay nanocomposite membranes with PEG 400 as a pore forming additive. *Desalination* **2012**, *286*, 131−137.

(19) Wan, L.-S.; Xu, Z.-K.; Wang, Z.-G. Leaching of PVP from polyacrylonitrile/PVP blending membranes: a comparative study of asymmetric and dense membranes. *J. Polym. Sci., Part B: Polym. Phys.* **2006**, *44*, 1490−1498.

(20) Mat Nawi, N. I.; Chean, H. M.; Shamsuddin, N. M.; Bilad, M. R.; Narkkun, T.; Faungnawaki, K.; Khan, A. L. Development of hydrophilic PVDF membrane using vapour induced phase separation method for produced water treatment. *Membranes* **2020**, *10*, No. 121.

(21) Fahrina, A.; Arahman, N.; Mulyati, S.; Aprilia, S.; Izati, N.; Mat, N.; Aqsha, A. R.; Takagi, R.; Matsuyama, H. Development of Polyvinylidene Fluoride Membrane by Incorporating Bio-Based Ginger Extract as Additive. *Polymers* **2020**, *12*, No. 2003.

(22) Bottino, A. Preparation and properties of novel organic−inorganic porous membranes. *Sep. Purif. Technol.* **2001**, *22*−*23*, 269−275.

(23) Mavukkandy, M. O.; Bilad, M. R.; Kujawa, J.; Al-Gharabli, S.; Arafat, H. A. On the effect of fumed silica particles on the structure, properties and application of PVDF membranes. *Sep. Purif. Technol.* **2017**, *187*, 365−373.

(24) Huang, J.; Zhang, K.; Wang, K.; Xie, Z.; Ladewig, B.; Wang, H. Fabrication of polyethersulfone-mesoporous silica nanocomposite ultrafiltration membranes with antifouling properties. *J. Membr. Sci.* **2012**, *423*−*424*, 362−370.

(25) Rosace, G.; Guido, E.; Colleoni, C.; Barigozzi, G. Influence of textile structure and silica based finishing on thermal insulation properties of cotton fabrics. *Int. J. Polym. Sci.* **2016**, 1−10.
(26) Rana, D.; Bag, S. K.; Bhattacharyya, N.; Mandal, B. M. Miscibility of poly (styrene-co-butyl acrylate) with poly (ethyl methacrylate): Existence of both UCST and LCST. *J. Polym. Sci., Part B: Polym. Phys.* **2000**, *38*, 369−375.
(27) Rana, D.; Mandal, B. M.; Bhattacharyya, S. N. Analogue Calorimetric Studies of Blends of Poly (vinyl ester) s and Polyacrylates. *Macromolecules* **1996**, *29*, 1579−1583.
(28) Tudu, B. K.; Sinhamahapatra, A.; Kumar, A. Surface modification of cotton fabric using TiO2 nanoparticles for self-cleaning, oil−water separation, antistain, anti-Water absorption, and antibacterial properties. *ACS Omega* **2020**, *14*, 7850−7860.
(29) Bravo, J.; Zhai, L.; Wu, Z.; Cohen, R. E.; Rubner, M. F. Transparent Superhydrophobic Films Based on Silica Nanoparticles. *Langmuir* **2007**, *23*, 7293−7298.
(30) Gutiérrez-Wing, C.; Hernández, R.; Mondragón-Galicia, G.; Villa-Sánchez, G.; Fernández-García, M. E.; Arenas-Alatorre; Mendoza-Anaya, D. A. J. Synthesis of silica−silver wires by a sol−gel technique. *Solid State Sci.* **2009**, *11*, 1722−1729.
(31) Rahman, I. A.; Padavettan, V. Synthesis of silica nanoparticles by sol-gel: size-dependent properties, surface modification, and applications in silica-polymer nanocomposites—A review, Hindawi Publishing Corporation. *J. Nanomater.* **2012**, No. 132424.
(32) Ochoa, M.; Lamy-Mendes, A.; Maia, A.; Portugal, A.; Luísa Durães, L. Influence of structure-directing additives on the properties of poly (methylsilsesquioxane) aerogel-Like materials. *Gels* **2019**, *5*, No. 6.
(33) Mansur, H.; Oréfice, R.; Pereira, M.; Lobato, Z.; Vasconcelos, W.; Machado, L. FTIR and UV-Vis study of chemically engineered biomaterial surfaces for protein immobilization. *Spectroscopy* **2002**, *16*, 351−360.
(34) Sriramulu, D.; Reed, L. E.; Annamalai, M.; Venkatesan, V. T.; Valiyaveettil, S. Synthesis and characterization of superhydrophobic, self-cleaning NIR-Reflective silica nanoparticles. *Sci. Rep.* **2016**, *6*, No. 35993.
(35) Pereira, M. M.; Neves, A. C.; Calvete, M. J. F.; Dias, L. D.; Fernandes, A. Binol derivative ligand immobilized onto silica: Alkyl-cyanohydrin synthesis via sequential hydroformylation/heterogeneous cyanosilylation reactions. *Catal. Today* **2013**, *218−219*, 99−106.
(36) Purcar, V.; Rădiţoiu, V.; Rădiţoiu, A.; Raduly, M.; Manea, R.; Frone, A.; Anastasescu, M.; CorneliaIspas, G.; Căprărescu, S. Bilayer coatings based on silica materials and iron (III) phthalocyanine − Sensitized TiO2 photocatalyst. *Mater. Res. Bull.* **2021**, *138*, No. 111222.
(37) Zhuang, J.; Li, M.; Yunqiao, P.; Ragauskas, A. J.; Yoo, C. G. Observation of potential contaminants in processed biomass using fourier transform infrared spectroscopy. *Appl. Sci.* **2020**, *10*, No. 4345.
(38) Viana, R. B.; Albérico, B. F.; Pimentel, S. A. Infrared spectroscopy of anionic, Cationic, and zwitterionic surfactants. *Adv. Phys. Chem.* **2012**, 1−14.
(39) Gautam, C.; Yadav, A. K.; Singh, A. K. A review on infrared spectroscopy of borate glasses with effects of different additives. *Int. Scholarly Res. Not.* **2012**, No. 428497.
(40) Petcu, C.; Purcar, V.; Spătaru, C.; et al. The influence of new hydrophobic silica nanoparticles on the surface properties of the films obtained from bilayer hybrids. *Nanomaterials* **2017**, *7*, No. 47.
(41) Yi, D.; Xu, C.; Tang, R.; et al. Synthesis of discrete Alkyl-Silica hybrid nanowires and their assembly into nanostructured super-hydrophobic membranes. *Angew. Chem., Int. Ed.* **2016**, *55*, 8375−8380.
(42) Amin, P. D.; Bhanushali, V.; Joshi, S. Role of Polyvinlyppyrrolidone in membrane technologies. *Int. J. ChemTech Res.* **2018**, *11*, 247−259.
(43) Rana, D.; Mandal, B. M.; Bhattacharyya, S. N. Analogue calorimetry of polymer blends: poly (styrene-co-acrylonitrile) and poly (phenyl acrylate) or poly(vinyl benzoate). *Polymer* **1996**, *37*, 2439−2443.
(44) Rana, D.; Mandal, B. M.; Bhattacharyya, S. N. Miscibility and phase diagrams of poly (phenyl acrylate) and poly(styrene-co-acrylonitrile) blends. *Polymer* **1993**, *34*, 1454−1459.

https://doi.org/10.1021/acsomega.1c04498
ACS Omega XXXX, XXX, XXX−XXX